

# Combining predictive distributions for statistical post-processing of ensemble forecasts

SÁNDOR BARAN<sup>1</sup> and SEBASTIAN LERCH<sup>2,3</sup>

<sup>1</sup>Faculty of Informatics, University of Debrecen

Kassai út 26, H-4028 Debrecen, Hungary

<sup>2</sup> Heidelberg Institute for Theoretical Studies

Schloss-Wolfsbrunnenweg 35, D-69118 Heidelberg, Germany

<sup>3</sup> Institute of Stochastics, Karlsruhe Institute of Technology,

Englerstraße 2, D-76128 Karlsruhe, Germany

February 9, 2019

## Abstract

Weather predictions typically take the form of forecast ensembles obtained from multiple runs of numerical weather prediction models with varying initial conditions and model physics. Due to systematic biases and errors in calibration, ensemble forecasts require some form of statistical post-processing. A standard approach is the ensemble model output statistics (EMOS) method, where a single parametric distribution with parameters depending on the ensemble members is used as forecast distribution. The success of this approach relies on finding and estimating appropriate parametric models for the weather quantity of interest, which, however, is a non-trivial task for weather variables such as wind speed or precipitation. In this article, a generally applicable and computationally efficient approach to combining forecast distributions from different EMOS models based on single parametric families is proposed. In four case studies with wind speed and precipitation forecasts from two different ensemble prediction systems, this approach outperforms standard combination approaches and performs similar to full mixture models while substantially reducing the computational costs.

*Key words:* ensemble model output statistics, ensemble post-processing, forecast combination, precipitation, probabilistic forecasting, wind speed.

# 1 Introduction

Nowadays, weather forecasts are usually based on the output of numerical weather prediction (NWP) models which describe the dynamical and physical behavior of the atmosphere through nonlinear partial differential equations. Single deterministic predictions produced by single runs of such models fail to account for uncertainties in the initial conditions and the numerical model. Therefore, NWP models are nowadays typically run several times with varying initial conditions and model physics, resulting in an ensemble of forecasts, see Palmer (2002) and Gneiting and Raftery (2005) for reviews. Examples of ensemble prediction systems (EPSs) are the 51-member European Centre for Medium-Range Weather Forecasts (ECMWF) ensemble (Molteni *et al.*, 1996), the eight-member University of Washington Mesoscale ensemble (UWME; Eckel and Mass, 2005), and the 11-member Aire Limitée Adaptation dynamique Développement International-Hungary Ensemble Prediction System (ALADIN-HUNEPS; Horányi *et al.*, 2006) of the Hungarian Meteorological Service (HMS). The transition from single deterministic forecasts to ensemble predictions can be seen as an important step towards probabilistic forecasting, however, ensemble forecasts are often underdispersive and subject to systematic bias. They thus require some form of statistical post-processing.

Over the past decade, various post-processing methods have been proposed in the meteorological literature. In the Bayesian model averaging (BMA; Raftery *et al.*, 2005) approach the forecast distribution is given by a weighted mixture of parametric densities, each of which depends on a single ensemble member with mixture weights being determined by the performance of the ensemble member in the training period. Within this article we build on the conceptually simpler ensemble model output statistics (EMOS) approach proposed by Gneiting *et al.* (2005), where the conditional distribution of the weather variable of interest given the ensemble predictions is modeled by a single parametric family. The parameters of the forecast distribution are connected to the ensemble forecast through suitable link functions. For example, the original EMOS approach models temperature with a Gaussian predictive distribution where the mean is an affine function of the ensemble forecasts, and the variance is an affine function of the ensemble variance.

Over the last years the EMOS approach has been extended to other weather variables such as wind speed (Thorarinsdottir and Gneiting, 2010; Lerch and Thorarinsdottir, 2013; Baran and Lerch, 2015; Scheuerer and Möller, 2015), precipitation (Scheuerer, 2014; Scheuerer and Hamill, 2015; Baran and Nemoda, 2016), and total cloud cover (Hemri *et al.*, 2016). The success of statistical post-processing relies on finding (and estimating) appropriate parametric families for the weather variable of interest. However, the choice of a suitable parametric model is a non-trivial task and often a multitude of competing models is available. The relative performance of these models usually varies for different data sets and applications.

The restriction to a single parametric family further limits the flexibility of the model.

Therefore, regime-switching combination and mixture model approaches have been proposed recently. In the regime-switching combination approach (Lerch and Thorarinsdottir, 2013) one of several candidate models is selected based on covariate information, whereas the mixture model approach of Baran and Lerch (2016) relies on jointly estimating the parameters and weight of a weighted mixture of two forecast distributions. However, the applicability of the regime-switching combination method is limited by the availability of suitable covariates, and the estimation of the mixture model is computationally demanding.

In this article we therefore propose a general, computationally efficient approach for combining forecast distributions from post-processing models. The proposed method is a two-step procedure where in a first step, the individual EMOS models based on single parametric distributions are estimated. In a second step the forecast distributions from the individual models are combined as a weighted mixture, where the optimal mixture weight is determined in a single step, usually involving numerical integration. Compared to the full mixture model approach of Baran and Lerch (2016), this new forecast combination method can be generally applied to any weather variable of interest given the availability of suitable component models, and it is computationally more efficient.

With a focus on wind speed and precipitation, we compare the new two-step combination approach to the full mixture model as well as standard forecast combination approaches that were recently applied in statistical post-processing (Gneiting and Ranjan, 2013; Möller and Groß, 2016). State of the art EMOS models are thereby used as mixture components. The different methods are compared in four case studies with wind speed and precipitation data from two ensemble prediction systems.

The remainder of this article is organized as follows. Section 2 contains a description of the ensembles and the observation data. In Section 3, the EMOS method is reviewed, and the individual EMOS models for wind speed and precipitation are introduced. Thereafter, a description of the novel two-step forecast combination approach and a short review of the spread-adjusted linear pool are provided. The various EMOS models and forecast combination approaches are compared in four case studies in Section 4. The article concludes with a discussion in Section 5.

## 2 Data

We consider two different weather variables, wind speed and precipitation accumulation, and two distinct data sets of ensemble forecast and corresponding validating observations for each weather quantity. The wind speed data sets are identical to data used in Baran and Lerch (2015, 2016), whereas the precipitation data coincide with those studied in Baran and Nemoda (2016). For detailed descriptions of the ensemble forecasts and corresponding observations we refer to these articles and references therein.

Ensemble members that are generated with the help of random perturbations of initial

conditions are statistically indistinguishable, and are referred to as exchangeable. The notion of exchangeability of ensemble members is important for the formulation of post-processing models, see Section 3 for details.

## 2.1 University of Washington mesoscale ensemble

The UWME covers the Pacific Northwest region of North America with a horizontal resolution of 12 km and consists of eight members generated from different runs of the fifth generation Pennsylvania State University–National Center for Atmospheric Research mesoscale model (Grell *et al.*, 1995). The initial and boundary conditions of the model runs are provided by different sources, the individual ensemble members can therefore be clearly distinguished and are considered to be non-exchangeable. The data set at hand contains 48 h ahead forecasts and corresponding validating observations for 10 m maximal wind speed (given in m/s) and 24 h precipitation accumulation (given in mm) for 152 stations in the Automated Surface Observing Network (National Weather Service, 1998) in the U.S. states of Washington, Oregon, Idaho, California and Nevada.

We focus on calendar year 2008 with additional forecasts and observations from the last months of 2007 used to allow for training periods of equal length for the model estimation. After removing days and locations with missing predictions and/or observations, 101 stations with wind speed and 83 stations with precipitation data remain, resulting in 27 481 and 20 522 individual forecast cases, respectively.

## 2.2 ALADIN-HUNEPS ensemble

The ALADIN-HUNEPS system of the HMS covering large parts of continental Europe on an 8 km grid is obtained with dynamical downscaling of the global ARPEGE based PEARP system of Météo France (Horányi *et al.*, 2011; Descamps *et al.*, 2015) and consists of 11 ensemble members, 10 of which are exchangeable forecasts from perturbed initial conditions and one control member from the unperturbed analysis.

We use ensembles of 42 h ahead forecasts of 10 m instantaneous wind speed (given in m/s) and 24 h precipitation accumulation (given in mm) issued for 10 major cities in Hungary together with the corresponding validation observations. Wind speed data are available for a one-year period from 1 April 2012 to 31 March 2013, and precipitation data are available between 1 October 2010 and 25 March 2011. Days with missing forecasts and/or observations are excluded from the analysis for both wind speed (6 days) and precipitation (2 days).

### 3 Ensemble model output statistics

Successful statistical post-processing of ensemble forecasts relies on finding (and estimating) appropriate parametric models for the conditional distribution of the weather variable of interest given the ensemble predictions. In case of the EMOS approach, the forecast distribution is given by a single parametric distribution with parameters depending on the ensemble forecast. While temperature can be modelled by a normal distribution where the mean and variance are affine functions of the ensemble predictions and ensemble variance, respectively (Gneiting *et al.*, 2005), the choice of a suitable parametric family is much less straightforward for weather variables such as wind speed or precipitation. A multitude of post-processing models and modeling strategies has been proposed over the last years. In the following short review, we focus on EMOS models for wind speed and precipitation, and subsequently propose a novel approach to combine forecast distributions from different models.

#### 3.1 EMOS models for wind speed

Non-negative weather variables such as wind speed require skewed predictive distributions with non-negative support such as Weibull (Justus *et al.*, 1978) or gamma distributions (Garcia *et al.*, 1988). Recently developed EMOS approaches utilize truncated normal (TN; Thorarinsdottir and Gneiting, 2010), gamma (Scheuerer and Möller, 2015), generalized extreme value (GEV; Lerch and Thorarinsdottir, 2013) and log-normal (LN; Baran and Lerch, 2015) distributions to model the conditional distribution of wind speed given the ensemble predictions. Here, we focus on the truncated normal and log-normal model.

##### 3.1.1 Truncated normal EMOS model

Denote by  $\mathcal{N}_0(\mu, \sigma^2)$  the TN distribution with location  $\mu$ , scale  $\sigma > 0$ , and cut-off at zero with probability density function (PDF)

$$g(x|\mu, \sigma) := \frac{\frac{1}{\sigma}\varphi((x-\mu)/\sigma)}{\Phi(\mu/\sigma)}, \quad \text{if } x \geq 0, \quad \text{and} \quad g(x|\mu, \sigma) := 0, \quad \text{otherwise,}$$

where  $\varphi$  and  $\Phi$  are the PDF and the cumulative distribution function (CDF) of the standard normal distribution, respectively. The predictive distribution of the EMOS model proposed by Thorarinsdottir and Gneiting (2010) is

$$\mathcal{N}_0(a_0 + a_1 f_1 + \dots + a_K f_K, b_0 + b_1 S^2) \quad \text{with} \quad S^2 := \frac{1}{K-1} \sum_{k=1}^K (f_k - \bar{f})^2, \quad (3.1)$$

where  $f_1, f_2, \dots, f_K$  denote the ensemble of distinguishable forecasts of wind speed for a given location and time, and  $\bar{f}$  is the ensemble mean. Location parameters  $a_0, a_1, \dots, a_K \in$

$\mathbb{R}$  and scale parameters  $b_0 \in \mathbb{R}$ ,  $b_1 \geq 0$  of model (3.1) can be estimated from the training data, consisting of ensemble members and verifying observations from the preceding  $n$  days, by optimizing an appropriate verification score, see Section 3.3.

However, most operational EPSs generate forecasts using random perturbations of the initial conditions resulting in statistically indistinguishable ensemble members which are referred to as exchangeable. Examples include the 51-member ECMWF ensemble, as well as multi-model EPSs such as the THORPEX Interactive Grand Global Ensemble (Swinbank *et al.*, 2016) or the GLAMEPS ensemble (Iversen *et al.*, 2011), which consist of several groups of exchangeable members. To account for the generation of the forecasts, ensemble members within a given group of exchangeable members should share the same coefficients in the post-processing model (Fraley *et al.*, 2010; Gneiting, 2014).

To formalize this notion, a generalized formulation of model (3.1) for the case of  $M$  ensemble members divided into  $K$  groups, where the  $k$ th group contains  $M_k \geq 1$  exchangeable ensemble members ( $\sum_{k=1}^K M_k = M$ ) introduced in Baran and Lerch (2015) is given by

$$\mathcal{N}_0\left(a_0 + a_1 \sum_{\ell_1=1}^{M_1} f_{1,\ell_1} + \cdots + a_K \sum_{\ell_K=1}^{M_K} f_{K,\ell_K}, b_0 + b_1 S^2\right).$$

Analogous concepts apply to all EMOS models discussed in the subsequent sections.

### 3.1.2 Log-normal EMOS model

As an alternative to the TN EMOS model, Baran and Lerch (2015) introduce an EMOS approach based on log-normal forecast distributions where the mean  $m$  and variance  $v$  of the predictive distribution are linked to the ensemble members as

$$m = \alpha_0 + \alpha_1 f_1 + \cdots + \alpha_K f_K \quad \text{and} \quad v = \beta_0 + \beta_1 S^2. \quad (3.2)$$

Obviously, these quantities uniquely determine the location  $\mu$  and shape  $\sigma > 0$  of the underlying LN distribution  $\mathcal{LN}(\mu, \sigma)$  with PDF

$$h(x|\mu, \sigma) := \frac{1}{x\sigma} \varphi((\log x - \mu)/\sigma), \quad \text{if } x \geq 0, \quad \text{and} \quad h(x|\mu, \sigma) := 0, \quad \text{otherwise,}$$

via transformations

$$\mu = \log\left(\frac{m^2}{\sqrt{v + m^2}}\right) \quad \text{and} \quad \sigma = \sqrt{\log\left(1 + \frac{v}{m^2}\right)}.$$

Similar to the TN EMOS model, estimates of parameters  $\alpha_0, \alpha_1, \dots, \alpha_K \in \mathbb{R}$  and  $\beta_0 \in \mathbb{R}$ ,  $\beta_1 \geq 0$  are obtained by optimizing the mean of an appropriate verification score over all forecast cases in the training data.

### 3.1.3 Combination and mixture models

The TN and LN models described above model the conditional distribution of wind speed given the ensemble predictions with a single parametric forecast distribution. This approach relies on the choice of a suitable parametric family, and limits the flexibility of the model. For instance, it can be demonstrated that the heavier tails of the LN model are more appropriate for modeling higher wind speeds in the right tail of the distribution, whereas the TN model is more appropriate for the bulk of the distribution, see Baran and Lerch (2016) for details.

Therefore, different combination and mixture models have been proposed in the literature. In the regime-switching combination approach (Lerch and Thorarinsdottir, 2013; Baran and Lerch, 2015) one of the candidate models is selected based on covariate information with suitably adapted parameter estimation procedures. For example, a TN model can be used if the median ensemble forecast is below a threshold  $\eta$ , and an LN model is used in case of median ensemble forecasts exceeding this threshold. Such combination models have been demonstrated to improve the predictive performance compared to the individual models, however, they require the choice of a suitable covariate, and the threshold parameter  $\eta$  has to be determined by repeating the model estimation over a grid of potential values, thereby limiting the flexibility and increasing the computational cost of such approaches.

In order to flexibly combine the advantages of lighter and heavier-tailed distributions and to avoid these problems in the process, Baran and Lerch (2016) propose a mixture model of the form

$$\psi(x | \mu_{TN}, \sigma_{TN}; \mu_{LN}, \sigma_{LN}; \omega) := \omega g(x | \mu_{TN}, \sigma_{TN}) + (1 - \omega)h(x | \mu_{LN}, \sigma_{LN}), \quad (3.3)$$

where the parameters of the component distributions depend on the ensemble forecasts as specified in (3.1) and (3.2). The EMOS coefficients and the weight  $\omega \in [0, 1]$  of the mixture model (3.3) are estimated jointly using optimum score estimation approaches. This mixture model approach results in significantly improved calibration (Baran and Lerch, 2016), however, it is computationally very demanding and does not allow for using standard optimum score estimation based on the continuous ranked probability score due to the lack of an analytic expression of the objective function, see Section 3.3 for details.

Compared to the joint estimation of all parameters in (3.3), the forecast combination approaches introduced in Sections 3.4 and 3.5 are two-step procedures where in a first step, EMOS models based on a single parametric family are estimated, and in a second step, these models are combined as a weighted mixture by estimating an appropriate weight. In Section 4 the full mixture model (3.3) is used as a benchmark, whereas the regime-switching combination approach will not be considered any further.

## 3.2 EMOS models for precipitation

The special discrete-continuous nature of precipitation requires a non-negative predictive distribution assigning positive mass to the event of zero precipitation. A popular choice is to consider a continuous distribution that can take both positive and negative values and left censor it at zero (Scheuerer, 2014; Scheuerer and Hamill, 2015; Baran and Nemoda, 2016), which thereby assigns the mass of negative values to zero precipitation accumulation.

### 3.2.1 Censored and shifted gamma EMOS model

Let  $G(\cdot|\kappa, \theta)$  denote the CDF of the  $\Gamma(\kappa, \theta)$  distribution with shape  $\kappa > 0$  and scale  $\theta > 0$  and let  $\delta > 0$ . Then the CDF of the shifted gamma distribution left censored at zero (CSG)  $\Gamma_0(\kappa, \theta, \delta)$  with shape  $\kappa$ , scale  $\theta$  and shift  $\delta$  is given by

$$G_0(x|\kappa, \theta, \delta) := G(x + \delta|\kappa, \theta), \quad \text{if } x \geq 0, \quad \text{and} \quad G_0(x|\kappa, \theta, \delta) := 0, \quad \text{otherwise,} \quad (3.4)$$

that is mass  $G(\delta|\kappa, \theta)$  is assigned to the origin. In the CSG EMOS approach of Baran and Nemoda (2016) the mean  $m = \kappa\theta$  and variance  $\sigma^2 = \kappa\theta^2$  of the uncensored gamma distribution  $\Gamma(\kappa, \theta)$  are affine functions of the ensemble and ensemble mean, respectively, that is

$$m = a_0 + a_1 f_1 + \cdots + a_K f_K \quad \text{and} \quad \sigma^2 = b_0 + b_1 \bar{f}. \quad (3.5)$$

### 3.2.2 Censored generalized extreme value EMOS model

The CDF of a GEV distribution  $\mathcal{G}\mathcal{E}\mathcal{V}(\mu, \sigma, \xi)$  with location  $\mu$ , scale  $\sigma > 0$  and shape  $\xi$  equals

$$H(x|\mu, \sigma, \xi) := \begin{cases} \exp\left(-\left[1 + \xi\left(\frac{x-\mu}{\sigma}\right)\right]^{-1/\xi}\right), & \xi \neq 0; \\ \exp\left(-\exp\left(-\frac{x-\mu}{\sigma}\right)\right), & \xi = 0, \end{cases} \quad \text{if } 1 + \xi(x - \mu)/\sigma > 0,$$

and zero otherwise, which for  $-0.278 < \xi < 1$  has a positive skewness and an existing mean

$$m = \begin{cases} \mu + \sigma \frac{\Gamma(1-\xi)-1}{\xi}, & \xi \neq 0; \\ \mu + \sigma\gamma, & \xi = 0, \end{cases}$$

where  $\gamma$  denotes the Euler-Mascheroni constant.

The EMOS model for precipitation accumulation proposed by Scheuerer (2014) is based on a censored GEV distribution  $\mathcal{G}\mathcal{E}\mathcal{V}_0(\mu, \sigma, \xi)$  with CDF

$$H_0(x|\mu, \sigma, \xi) = H(x|\mu, \sigma, \xi), \quad \text{if } x \geq 0, \quad \text{and} \quad H_0(x|\mu, \sigma, \xi) := 0, \quad \text{otherwise,} \quad (3.6)$$

where

$$m = \alpha_0 + \alpha_1 f_1 + \cdots + \alpha_K f_K + \nu p_0 \quad \text{and} \quad \sigma = \beta_0 + \beta_1 \text{MD}(f), \quad (3.7)$$



with

$$p_0 := \frac{1}{K} \sum_{k=1}^K \mathbb{1}_{\{f_k=0\}} \quad \text{and} \quad \text{MD}(f) := \frac{1}{K^2} \sum_{k,\ell=1}^K |f_k - f_\ell|,$$

where  $\mathbb{1}_A$  denotes the indicator function of the set  $A$ .

### 3.2.3 Mixture models

Similar to wind speed, general mixture models with CSG and GEV component distributions of the form

$$\varrho(x | \kappa, \theta, \delta; \mu, \sigma, \xi; \omega) := \omega g_0(x | \kappa_{CSG}, \theta_{CSG}, \delta_{CSG}) + (1 - \omega) h_0(x | \mu_{GEV}, \sigma_{GEV}, \xi_{GEV}), \quad (3.8)$$

can be formulated, where  $g_0(\cdot | \kappa, \theta, \delta)$  and  $h_0(\cdot | \mu, \sigma, \xi)$  denote the generalized PDFs of the CSG and censored GEV distributions, respectively, and the dependence of parameters  $\kappa_{CSG}, \theta_{CSG}$  and  $\mu_{GEV}, \sigma_{GEV}$  on the ensemble is given by (3.5) and (3.7).

However, joint optimum score estimation of the parameters is even more involved than in the case of the TN-LN mixture model (3.3) for wind speed due to the larger number of parameters and the discrete-continuous nature of the forecast distribution  $\varrho$ . As initial tests with the precipitation data sets introduced in Section 2 indicated problematic behavior of the numerical optimization algorithms potentially caused by the non-smooth dependence of the objective functions on the parameters, we do not pursue this approach any further and only consider the two-step forecast combination approaches introduced in Sections 3.4 and 3.5.

## 3.3 Forecast evaluation and parameter estimation

In probabilistic forecasting the general aim is to maximize the sharpness of the predictive distribution subject to calibration (Gneiting *et al.*, 2007). Calibration refers to the statistical consistency between the forecast and the observation, and given that the predictive distribution is calibrated, it should be as concentrated (or sharp) as possible. Calibration and sharpness can be assessed simultaneously with the help of proper scoring rules.

Proper scoring rules are loss functions that assign a numerical value to pairs of forecasts and observations. In atmospheric sciences the most popular scoring rules are the continuous ranked probability score (CRPS; Matheson and Winkler, 1976; Gneiting and Raftery, 2007) and the logarithmic score (LogS; Good, 1952). Given a predictive CDF  $F(y)$  and an

observation  $x$ , the CRPS is defined as

$$\begin{aligned} \text{CRPS}(F, x) &:= \int_{-\infty}^{\infty} (F(y) - \mathbb{1}_{\{y \geq x\}})^2 dy \\ &= \int_{-\infty}^x F^2(y) dy + \int_x^{\infty} (1 - F(y))^2 dy \\ &= \mathbb{E}|X - x| - \frac{1}{2}\mathbb{E}|X - X'|, \end{aligned} \tag{3.9}$$

where  $X$  and  $X'$  are independent random variables with CDF  $F$  and finite first moment. The last representation in (3.9) implies that the CRPS can be expressed in the same unit as the observation. The logarithmic score is the negative logarithm of the predictive density  $f(y)$  evaluated at the verifying observation, i.e.,

$$\text{LogS}(F, x) := -\log(f(x)).$$

Both CRPS and LogS are proper scoring rules (Gneiting and Raftery, 2007) which are negatively oriented, that is, smaller scores indicate better forecasts.

Proper scoring rules provide valuable tools for the estimation of model parameters. Following the general optimum score estimation approach of Gneiting and Raftery (2007), the parameters of a predictive distribution can be determined by optimizing the average value of a proper scoring rule as a function of the parameters over a suitably chosen training set. Optimum score estimation based on minimizing the LogS then corresponds to classical maximum likelihood (ML) estimation. If closed form expressions of the integral in (3.9) are available, minimum CRPS estimation, i.e. optimum score estimation based on minimizing the mean CRPS, often provides a valuable, more robust alternative to ML estimation. In recent applications to statistical post-processing of ensemble forecasts, minimum CRPS estimation has been demonstrated to lead to slightly better predictive performance, see e.g. Baran and Lerch (2016); Baran and Nemoda (2016).

Analytic expressions of the CRPS are available for all individual EMOS models for wind speed and precipitation introduced in Sections 3.1 and 3.2, thereby allowing for efficient parameter estimation procedures by minimizing the mean CRPS over the forecast cases in the training periods. The closed form solutions are provided in the corresponding articles (Thorarinsdottir and Gneiting, 2010; Baran and Lerch, 2015; Scheuerer, 2014; Scheuerer and Hamill, 2015). Implementations for the statistical programming language R (R Core Team, 2016) are for example available in the `scoringRules` package (Jordan *et al.*, 2016). The parameter estimation for the EMOS models is performed using the Broyden-Fletcher-Goldfarb-Shanno (BFGS) algorithm (Press *et al.*, 2007, Section 10.9) implemented in the `optim` function in R. In the case of precipitation we use a constrained version of the BFGS algorithm to ensure positivity of the EMOS coefficients. See Section 4 for details on the selection of the training sets over which the parameters are estimated.

By contrast, the CRPS is not available in closed form for the mixture models (3.3) and (3.8), so each step of the optimization procedure based on minimizing the CRPS re-

quires a numerical integration resulting in very high computational costs. Therefore, we do not consider minimum CRPS estimation for these mixture models and use ML estimation of the parameters instead. In case of the mixture model (3.3) for wind speed, this approach leads to similar predictive performance compared to minimum CRPS estimation, see Baran and Lerch (2016) for details. However, the analogous mixture model (3.8) for precipitation can not be successfully estimated, as both the BFGS and the more robust Nelder and Mead (1965) algorithm encounter numerical issues, do not converge, or fail to give reasonable parameter estimates. Potential reasons for these problems include the large dimensions of the optimization problem, the non-smooth character of the likelihood function, as well as the challenging discrete-continuous nature of the predictive distribution.

### 3.4 Forecast combination

We propose a computationally efficient two-step procedure for estimating the parameters of mixture models consisting of two different families of distributions. The first step is given by the estimation of component models in the form of EMOS models based on suitable single parametric families. In a second step, the component models are combined by estimating the mixture weight. Compared to the previously discussed mixture model (3.3), this two-step approach is computationally much more efficient as it reduces the dimensionality of the optimization problems. Further, this approach can be flexibly applied to any weather variable of interest given that suitable component models are available, therefore, the model formulation is given in a general form. The EMOS models introduced in Sections 3.1 and 3.2 are later used as component distributions for wind speed and precipitation, respectively.

Let  $G(x|\mathbf{f};\nu)$  and  $H(x|\mathbf{f};\theta)$  be predictive CDFs belonging to two different families of distributions depending on the ensemble  $\mathbf{f}$  via parameters  $\nu$  and  $\theta$ , respectively, and let  $(x_k, \mathbf{f}_k)$ ,  $k = 1, 2, \dots, n$ , denote the pairs of verifying observations and ensemble forecasts in the training data. Consider a mixture model with predictive CDF of the general form

$$\Psi(x|\mathbf{f};\nu,\theta,\omega) := \omega G(x|\mathbf{f};\nu) + (1-\omega)H(x|\mathbf{f};\theta), \quad \omega \in [0,1]. \quad (3.10)$$

Short calculation based on the integral representation in the second line of (3.9) shows

$$\begin{aligned} \text{CRPS}(\Psi(\cdot|\mathbf{f};\nu,\theta,\omega),x) &= \omega^2 \text{CRPS}(G(\cdot|\mathbf{f};\nu),x) + (1-\omega)^2 \text{CRPS}(H(\cdot|\mathbf{f};\theta),x) \\ &+ 2\omega(1-\omega) \left[ \int_{-\infty}^x G(y|\mathbf{f};\nu)H(y|\mathbf{f};\theta)dy + \int_x^{\infty} (1-G(y|\mathbf{f};\nu))(1-H(y|\mathbf{f};\theta))dy \right]. \end{aligned}$$

In a first step, the mixture components given by the EMOS models based on single parametric families are estimated. Let  $\nu_\circ$  and  $\theta_\circ$  denote the optimal parameters of the individual models in the training set, that is

$$\nu_\circ := \arg \min_{\nu} \overline{\text{CRPS}(G,\nu)} \quad \text{and} \quad \theta_\circ := \arg \min_{\theta} \overline{\text{CRPS}(H,\theta)},$$

where

$$\overline{\text{CRPS}(G, \nu)} := \frac{1}{n} \sum_{k=1}^n \text{CRPS}(G(\cdot | \mathbf{f}_k; \nu), x_k), \quad \overline{\text{CRPS}(H, \theta)} := \frac{1}{n} \sum_{k=1}^n \text{CRPS}(H(\cdot | \mathbf{f}_k; \theta), x_k).$$

In case of individual EMOS models presented in Sections 3.1 and 3.2 these estimates can easily be computed as described in Section 3.3. We propose to use  $\nu_o$  and  $\theta_o$  as parameters of the mixture model (3.10) and then, as a second step, to optimize

$$\overline{\text{CRPS}(\Psi, \omega)} := \frac{1}{n} \sum_{i=1}^n \text{CRPS}(\Psi(\cdot | \mathbf{f}_k; \nu_o, \theta_o, \omega), x_k)$$

as a function of  $\omega$ . The minimum point of  $\overline{\text{CRPS}(\Psi, \omega)}$  is obviously

$$\omega_o^* = \frac{\overline{\text{CRPS}(H, \theta_o)} - \overline{\mathcal{M}(G, H, \nu_o, \theta_o)}}{\overline{\text{CRPS}(G, \nu_o)} + \overline{\text{CRPS}(H, \theta_o)} - 2\overline{\mathcal{M}(G, H, \nu_o, \theta_o)}},$$

where

$$\overline{\mathcal{M}(G, H, \nu, \theta)} := \frac{1}{n} \sum_{k=1}^n \left[ \int_{-\infty}^{x_k} G(y | \mathbf{f}_k; \nu) H(y | \mathbf{f}_k; \theta) dy + \int_{x_k}^{\infty} (1 - G(y | \mathbf{f}_k; \nu)) (1 - H(y | \mathbf{f}_k; \theta)) dy \right],$$

and short calculation shows

$$\begin{aligned} \omega_o^* &= \frac{\sum_{k=1}^n \int_{-\infty}^{\infty} H(y | \mathbf{f}_k; \theta_o) (H(y | \mathbf{f}_k; \theta_o) - G(y | \mathbf{f}_k; \nu_o)) dy}{\sum_{k=1}^n \int_{-\infty}^{\infty} (H(y | \mathbf{f}_k; \theta_o) - G(y | \mathbf{f}_k; \nu_o))^2 dy} \\ &\quad - \frac{\sum_{k=1}^n \int_{x_k}^{\infty} (H(y | \mathbf{f}_k; \theta_o) - G(y | \mathbf{f}_k; \nu_o)) dy}{\sum_{k=1}^n \int_{-\infty}^{\infty} (H(y | \mathbf{f}_k; \theta_o) - G(y | \mathbf{f}_k; \nu_o))^2 dy}. \end{aligned}$$

Now, as  $\omega_o^*$  might fall outside the unit interval  $[0, 1]$ , we use

$$\omega_o := \min \{ \max \{ 0, \omega_o^* \}, 1 \}$$

as a definite estimate of the weight. Finally, one can easily show that within the training sample

$$\overline{\text{CRPS}(\Psi, \omega_o)} \leq \min \{ \overline{\text{CRPS}(G, \nu_o)}, \overline{\text{CRPS}(H, \theta_o)} \}, \quad (3.11)$$

so the mean CRPS of the mixture model (3.10) with parameters  $(\nu_o, \theta_o, \omega_o)$  cannot exceed the optimal mean CRPS values of the components. Obviously, (3.11) gives no guarantee that for a new out-of-sample pair  $(\tilde{x}, \tilde{\mathbf{f}})$  the CRPS of the mixture  $\text{CRPS}(\Psi(\cdot | \tilde{\mathbf{f}}; \nu_o, \theta_o, \omega_o), \tilde{x})$  does not exceed any of the corresponding individual CRPS values. However, in the case studies presented in Section 4 the mixture models show significant improvements in predictive performance compared to the models based on single parametric families. Compared to the mixture model approach for wind speed proposed by Baran and Lerch (2015) discussed in Section 3.1, the new two-step method displays similar predictive performance, but significantly reduces the computational costs.

The above method can be generalized to a convex combination of  $r$  different parametric families. However, in this case the optimal weight vector is a coordinate-wise non-negative solution of a quadratic optimization problem with a single linear constraint, where the main diagonal of the corresponding  $r \times r$  symmetric matrix consists of the mean CRPS values of the component models, whereas the other entries, which are similar to  $\overline{\mathcal{M}(G, H, \nu, \theta)}$ , can be expressed via integrals.

### 3.5 Spread-adjusted linear combination approach

Following the lead of Möller and Groß (2016), we introduce linear pooling and spread-adjusted linear pooling of predictive distributions as a benchmark approach to forecast combination for statistical post-processing. Given two predictive distributions  $G(x|\mathbf{f};\nu)$  and  $H(x|\mathbf{f};\theta)$ , with notation as in Section 3.4, the forecast distribution of the spread-adjusted linear pool (SLP) combined predictive distribution (Gneiting and Ranjan, 2013) with spread adjustment parameter  $c > 0$  takes the form

$$F^{\text{SLP}}(x|\mathbf{f};\nu,\theta,\omega) := \omega G\left(\frac{x}{c}|\mathbf{f};\nu\right) + (1-\omega)H\left(\frac{x}{c}|\mathbf{f};\theta\right), \quad \omega \in [0,1]. \quad (3.12)$$

The traditional linear pool (LP) is obtained for  $c = 1$ . As demonstrated by Gneiting and Ranjan (2013), linear pooling of predictive distributions increases the dispersion of the forecasts, whereas the SLP approach allows to correct for this deficiency.

We use the spread-adjusted linear pool to combine the EMOS models based on single parametric families for both wind speed and precipitation in a two-step procedure. Following Möller and Groß (2016), the SLP parameters  $\omega \in [0,1]$  and  $c > 0$  are determined by applying the combination formula (3.12) for all 273 possible combinations of candidate parameter values  $\omega \in \{0, 0.05, \dots, 0.95, 1\}$  and  $c \in \{0.7, 0.75, \dots, 1.25, 1.3\}$  during the training periods of the corresponding EMOS models, and selecting the parameter values resulting in the lowest mean CRPS in the training sample. As initial tests indicated improvements in the predictive performance, we further employ the traditional linear pool by fixing  $c = 1$  and selecting the optimal weight  $\omega \in \{0, 0.05, \dots, 0.95, 1\}$  as described above.

The LP and the combination approach described in Section 3.4 therefore differ in the way the weights  $\omega$  are determined. While the weights in the combination approach (3.10) are computed as minimum point of  $\overline{\text{CRPS}(\Psi, \omega)}$  and require only a single numerical integration step to obtain  $\overline{\mathcal{M}(G, H, \nu, \theta)}$ , the LP approach requires repeated numerical integrations to obtain CRPS values for all possible choices of the weight parameter and thus it is computationally more demanding.

The SLP combination formula (3.12) can be further generalized by allowing for different spread adjustment parameters in the components (Gneiting and Ranjan, 2013), however, this leads to even higher computational costs and is not feasible for the data sets investigated here.

## 4 Case studies

Here, we report the results of four case studies for the wind speed and precipitation data sets introduced in Section 2.

### 4.1 Forecast verification

The calibration of the raw ensemble and the post-processed forecasts can be assessed graphically with the help of verification rank and probability integral transform (PIT) histograms, respectively. The former is the histogram of ranks of the validating observations with respect to the corresponding ensemble predictions computed for all forecast cases (see e.g. Wilks, 2011, Section 7.7.2), where in case of precipitation accumulation zero observations are randomized among all zero forecasts. For a calibrated ensemble, the observations and the ensemble forecasts should be exchangeable, resulting in a uniform verification rank histogram. The PIT is the value of the predictive CDF evaluated at the verifying observation (Raftery *et al.*, 2005), PIT histograms can therefore be seen as continuous counterparts of verification rank histograms. To account for the discrete-continuous nature of the models for precipitation accumulation, in case of zero observed precipitation a random value is chosen uniformly from the interval between zero and the probability of no precipitation (Sloughter *et al.*, 2007). The visual inspection of deviations from the desired uniform distribution of the verification ranks and PIT values allows to further detect possible reasons of miscalibration (Gneiting *et al.*, 2007).

Apart from the visual inspection of PIT histograms, formal statistical test of uniformity of the PIT values can be used to assess calibration. Here we apply the classical Kolmogorov-Smirnov test, however, alternative tests that account for the complex dependence structures in PIT values of sequential k-step-ahead forecasts have been proposed in the econometric literature, see Baran and Lerch (2016) and references therein for details.

Numerical measures of calibration and sharpness are provided by coverage and width of prediction intervals. The coverage of an  $(1-\alpha)100\%$ ,  $\alpha \in (0, 1)$ , central prediction interval is the proportion of validating observations located between the lower and upper  $\alpha/2$  quantiles of the predictive distribution and should be around  $(1-\alpha)100\%$  for a calibrated forecast distribution. Sharper predictive distributions correspond to narrower prediction intervals. Choosing  $(1-\alpha)100\%$  to match the nominal coverage of the ensemble allows to directly compare the calibration of the raw ensemble and the post-processed forecast distributions. Due to the discrete-continuous nature of forecast distributions, in the case of precipitation the computation of coverage of the prediction intervals has to be adjusted. If the central prediction interval is concentrated in the origin and the corresponding observation is zero as well, the inclusion of the observation is chosen randomly according to the nominal coverage (UWME: 7/9; ALADIN-HUNEPS: 10/12).

As noted in Section 3.3, proper scoring rules are valuable tools for simultaneously evalu-

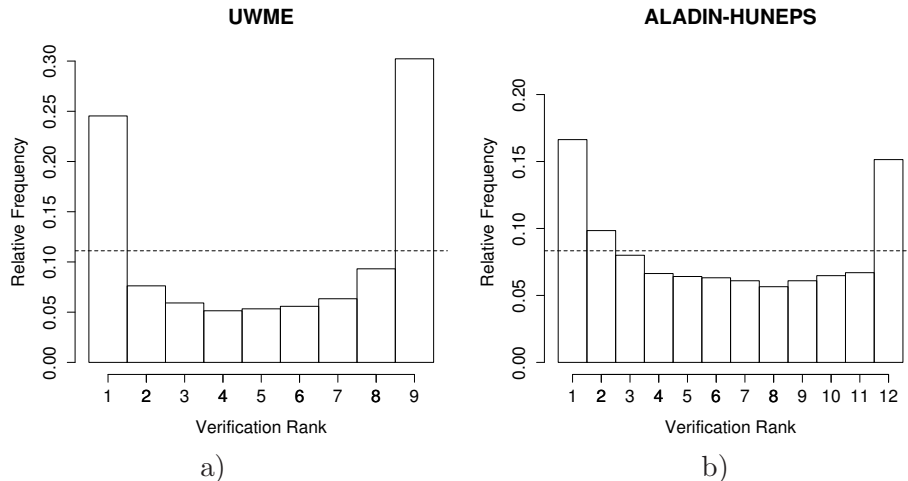


Figure 1: Verification rank histograms for wind speed over the verification periods. a) UWME for the calendar year 2008; ALADIN-HUNEPS ensemble for the period 15 May 2012 – 31 March 2013.

ating the calibration and sharpness of forecast distributions. Here, we use the CRPS (3.9), as well as the absolute error (AE)

$$\text{AE}(\hat{x}, x) := |\hat{x} - x|,$$

where the point forecast  $\hat{x}$  is given by the median of the forecast distribution, and  $x$  denotes the validating observation. The deterministic accuracy of the point forecasts is evaluated using the mean absolute error (MAE) over the forecast cases in the verification period.

## 4.2 Wind speed

The post-processing models introduced in Section 3 are estimated using the optimum score estimation approach described in Section 3.3. The TN and LN component models are estimated by minimizing the mean CRPS over the training sets, whereas ML estimation is employed for the full mixture model (3.3). Following previous work (Baran and Lerch, 2015, 2016), we use rolling training periods of length 30 days (UWME data) and 43 days (ALADIN-HUNEPS data), and estimate the parameters regionally by combining forecast cases from all available observation stations to form a single training set for all stations. Note that alternative similarity-based semi-local approaches to selecting the training sets have recently been investigated by Lerch and Baran (2016).

Given the estimates of the component models, the weight in the two-step combination approach and the SLP parameters are estimated over the corresponding rolling training periods as described in Sections 3.4 and 3.5, respectively. For the first day in the verification period, the SLP parameters are set to  $w = 0.5$  and  $c = 1$  since no corresponding past

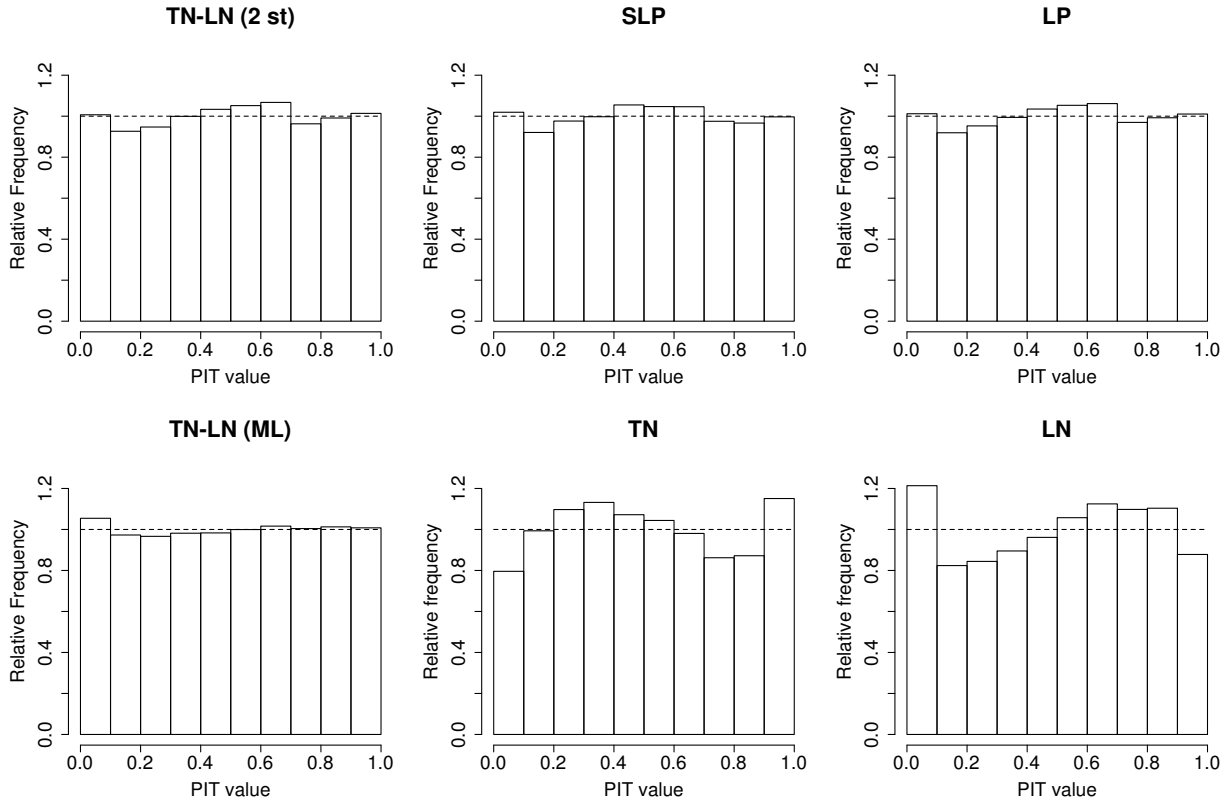


Figure 2: PIT histograms of post-processed forecasts for wind speed for the UWME for the verification period given by the calendar year 2008.

	Wind speed					
	TN-LN (2 st)	SLP	LP	TN-LN (ML)	TN	LN
UWME (mean $p$ )	0.304	0.348	0.298	0.473	0.042	0.007
ALADIN-HUNEPS	0.506	0.604	0.341	0.570	0.127	$3.8 \times 10^{-6}$
	Precipitation accumulation					
	CSG-GEV	SLP	LP	CSG	GEV	
UWME (mean $p$ )	0.180	0.278	0.292	0.075	0.384	
ALADIN-HUNEPS	0.430	0.002	0.123	0.097	0.711	

Table 1:  $p$ -values of Kolmogorov-Smirnov tests of uniformity of the PIT values. Means of 10 000 random samples of sizes 2 500 each for the UWME data, individual  $p$ -values for the ALADIN-HUNEPS data.

forecast cases are available. For the following days, the training sets are expanded until rolling training sets of the full length become available.

Verification rank histograms for the two ensembles are shown in Figure 1. The U-shaped histograms indicate underdispersive forecast distributions with too many observations falling



Forecast	CRPS (m/s)	MAE (m/s)	Coverage (%)	Av.width (m/s)
TN-LN (2 st)	1.111	1.549	77.60	4.607
SLP	1.115	1.553	77.84	4.637
LP	1.111	1.549	77.57	4.612
TN-LN (ML)	1.100	1.549	77.08	4.650
TN	1.114	1.550	78.65	4.666
LN	1.113	1.553	76.92	4.639
Ensemble	1.353	1.655	45.24	2.532

Table 2: Mean CRPS of probabilistic forecasts, MAE of median forecasts and coverage and average width of 77.78 % central prediction intervals for wind speed for the UWME data.

Forecast	TN-LN (2 st)	SLP	LP	TN-LN (ML)	TN	LN	Ensemble
TN-LN (2 st)	–	<b>-4.871</b>	-1.393	<b>13.641</b>	<b>-11.485</b>	<b>-9.753</b>	<b>-61.046</b>
SLP	<b>2.814</b>	–	<b>4.794</b>	<b>12.406</b>	1.262	<b>2.121</b>	<b>-57.935</b>
LP	<b>-2.792</b>	<b>-3.192</b>	–	<b>13.525</b>	<b>-10.967</b>	<b>-8.737</b>	<b>-61.112</b>
TN-LN (ML)	-0.475	<b>-2.796</b>	0.022	–	<b>-15.543</b>	<b>-15.726</b>	<b>-60.236</b>
TN	1.904	-1.675	<b>2.448</b>	1.506	–	1.500	<b>-60.571</b>
LN	<b>7.018</b>	0.159	<b>7.361</b>	<b>4.558</b>	<b>2.374</b>	–	<b>-59.899</b>
Ensemble	<b>23.092</b>	<b>21.516</b>	<b>23.304</b>	<b>22.233</b>	<b>23.178</b>	<b>21.541</b>	–

Table 3: Values of the test statistics of the DM test for equal predictive performance based on the CRPS (*upper triangle*) and the AE of the median forecast (*lower triangle*) for wind speed for the UWME data. Negative/positive values indicate a superior predictive performance of the forecast given in the row/column label, bold numbers correspond to values of the test statistic that are significant at the 0.05 level.

outside the range of the ensemble, and illustrate the potential for improvement through post-processing.

#### 4.2.1 University of Washington mesoscale ensemble

PIT histograms for all post-processing models are shown in Figure 2. Compared to the verification rank histogram of the raw ensemble forecasts in Figure 1a, all post-processing approaches are better calibrated, which is indicated by smaller deviations from the desired uniform distribution of the PIT values. The calibration of the individual TN and LN component models is not perfect, with the TN model showing systematic over-predictions of high wind speeds, and the LN model over-predicting low wind speed values. By contrast, the three forecast combination approaches (TN-LN (2 st), SLP and LP) and the full mixture model (TN-LN (ML)) are able to correct for these deficiencies and are well calibrated.

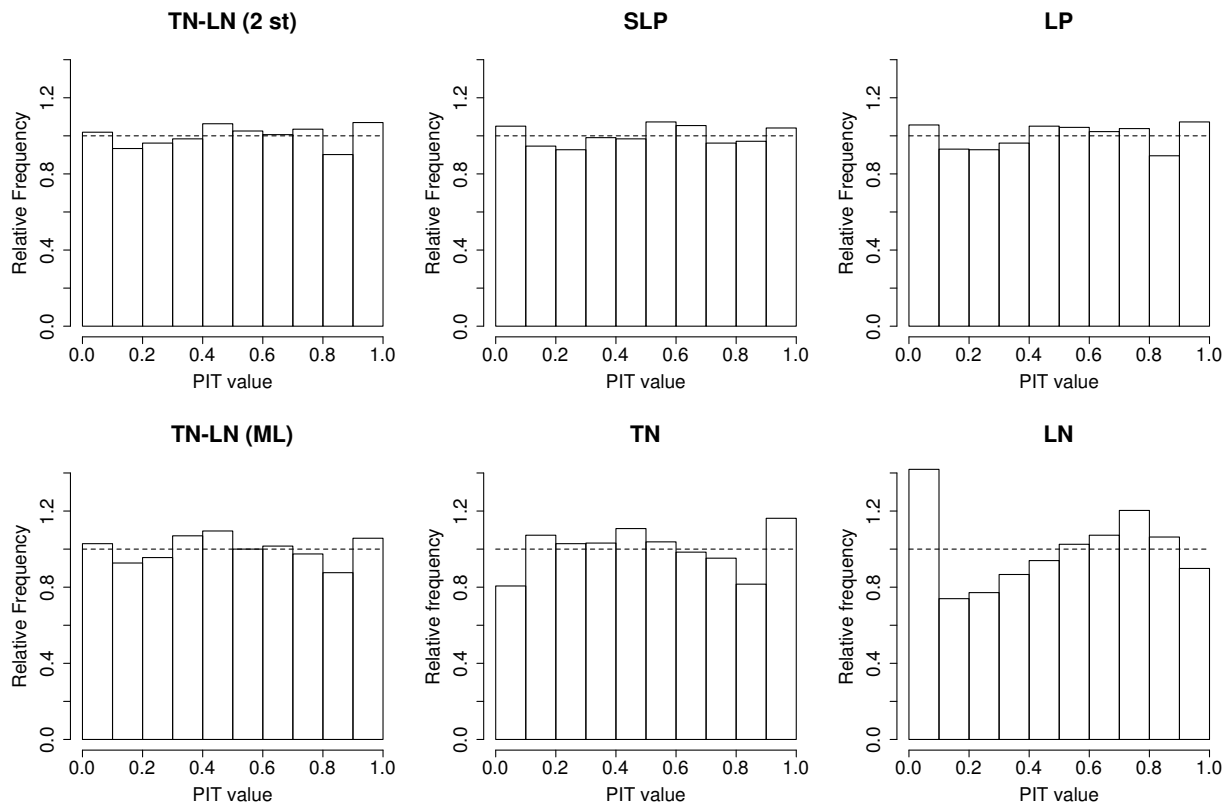


Figure 3: PIT histograms of post-processed forecasts for wind speed for the ALADIN-HUNEPS ensemble for the verification period 15 May 2012 – 31 March 2013.

The visual impressions from the PIT histograms in Figure 2 are substantiated by the  $p$ -values of Kolmogorov-Smirnov tests of uniformity of the PIT values reported in Table 1. While the null hypothesis of uniformity is rejected for the TN and LN models, this is not the case for the combination and mixture approaches. Note that due to the large sample size and our focus on comparative assessment of calibration, we compute mean  $p$ -values from smaller random sub-samples, see Baran and Lerch (2016) for details.

The verification scores for the different methods are summarized in Table 2. All post-processing models clearly outperform the raw ensemble forecasts by a wide margin. Among the different approaches, the best results are obtained for the full TN-LN mixture model (3.3), followed by the new TN-LN two-step combination model and the LP approach. The SLP model fails to outperform the individual TN and LN component models and shows the worst predictive performance.

To assess the statistical significance of these findings, two-sided Diebold-Mariano (DM; Diebold and Mariano, 1995) tests of equal predictive performance are performed, which allow to account for dependence in the forecast errors, see Baran and Lerch (2015) for details. The results are presented in Table 3 containing the values of the DM test statistics based on the CRPS and the AE for all pair-wise comparisons of forecasts. Almost all observed score

Forecast	CRPS (m/s)	MAE (m/s)	Coverage (%)	Av.width (m/s)
TN-LN (2 st)	0.737	1.035	82.48	3.518
SLP	0.741	1.041	84.41	3.537
LP	0.738	1.035	82.38	3.521
TN-LN (ML)	0.734	1.036	82.35	3.551
TN	0.738	1.037	83.56	3.534
LN	0.741	1.038	80.41	3.566
Ensemble	0.803	1.069	68.22	2.884

Table 4: Mean CRPS of probabilistic forecasts, MAE of median forecasts and coverage and average width of 83.33% central prediction intervals for wind speed for the ALADIN-HUNEPS ensemble.

Forecast	TN-LN (2 st)	SLP	LP	TN-LN (ML)	TN	LN	Ensemble
TN-LN (2 st)	–	<b>-2.789</b>	<b>-2.322</b>	<b>2.454</b>	-1.629	<b>-3.337</b>	<b>-12.834</b>
SLP	<b>2.845</b>	–	<b>2.419</b>	<b>3.747</b>	1.944	-0.225	<b>-11.688</b>
LP	0.554	<b>-2.671</b>	–	<b>2.827</b>	-0.569	<b>-3.096</b>	<b>-12.696</b>
TN-LN (ML)	0.265	-1.571	0.155	–	<b>-2.788</b>	<b>-4.971</b>	<b>-12.928</b>
TN	1.560	-1.695	1.101	0.478	–	<b>-2.013</b>	<b>-12.661</b>
LN	1.427	-0.866	1.402	0.865	0.451	–	<b>-11.830</b>
Ensemble	<b>4.493</b>	<b>3.566</b>	<b>4.420</b>	<b>4.362</b>	<b>4.347</b>	<b>3.717</b>	–

Table 5: Values of the test statistics of the DM test for equal predictive performance based on the CRPS (*upper triangle*) and the AE of the median forecast (*lower triangle*) for wind speed for the ALADIN-HUNEPS data. Negative/positive values indicate a superior predictive performance of the forecast given in the row/column label, bold numbers correspond to values of the test statistic that are significant at the 0.05 level.

differences are significant at the 0.05 level, specifically, the new two-step combination approach significantly outperforms the TN, LN and SLP models, whereas the CRPS differences to the LP model are not significant. In terms of AE, the SLP model is outperformed by all competing post-processing approaches but the LN model. This observation can potentially be explained by the finite grid over which the SLP parameters are estimated which limits the possible choice of parameter values, but is necessary for computational reasons.

#### 4.2.2 ALADIN-HUNEPS ensemble

The PIT histograms for the post-processed forecasts for the ALADIN-HUNEPS ensemble shown in Figure 3 resemble the shapes of the histograms of the corresponding models for the UWME data, and point to similar miscalibration of the TN and LN models. Again, all combination and mixture models are able to correct for the systematic errors in calibration

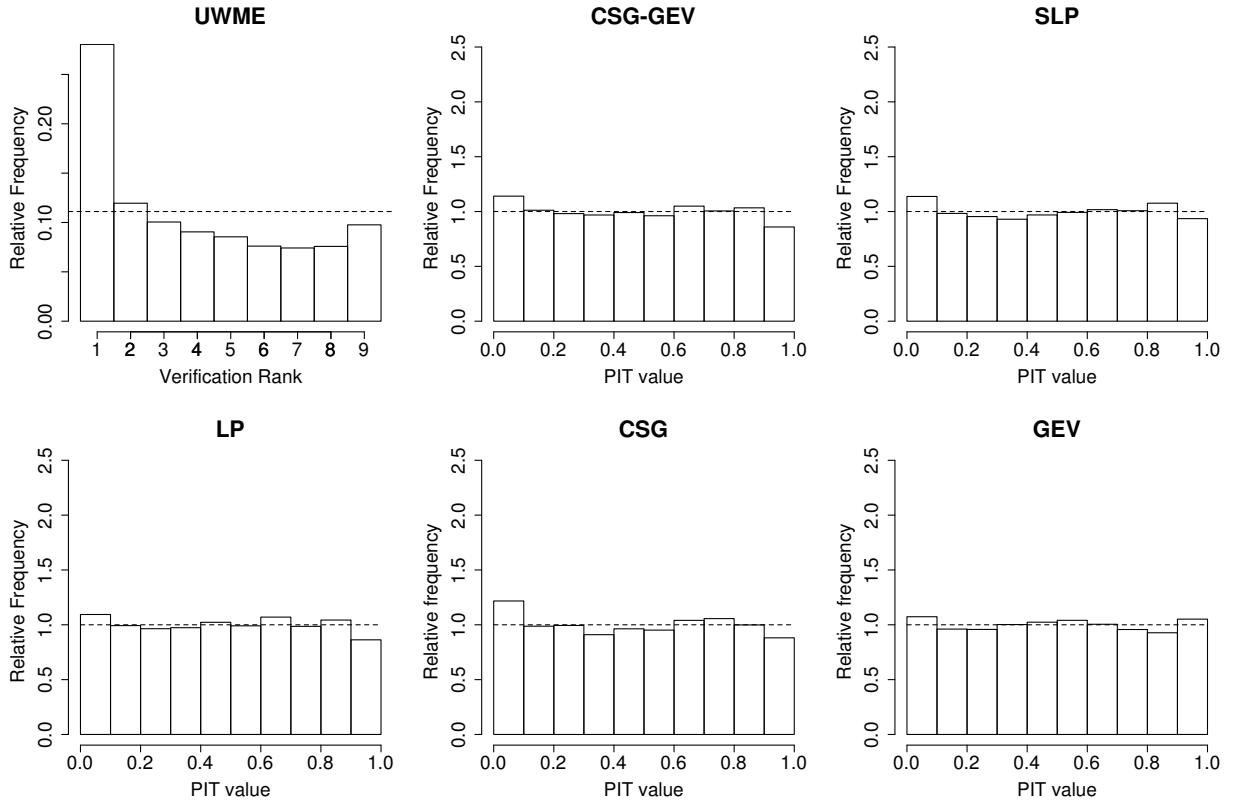


Figure 4: Verification rank histogram of the raw ensemble and PIT histograms of post-processed forecasts for precipitation accumulation for the UWME for the verification period given by calendar year 2008.

and show clearly smaller deviations from the desired uniform distribution, indicating better calibrated forecast distributions.

The verification scores reported in Table 4 result in similar rankings of the post-processing approaches as for the UWME data. The TN and LN component models are outperformed by all competitors except for the SLP approach. The best results are obtained for the full mixture model (3.3), closely followed by the two-step combination approach and the LP model. As indicated by the values of the DM test statistic summarized in Table 5, most of the CRPS differences are significant, specifically, the novel two-step combination approach significantly outperforms the LP model.

### 4.3 Precipitation

Similar to wind speed, the post-processing models introduced in Section 3 are estimated using optimum score estimation approaches. The coefficients of the EMOS models (3.4) and (3.6) based on single CSG and GEV distributions are obtained using rolling training periods of lengths 70 (UWME) and 55 days (ALADIN-HUNEPS), which ensures comparability with

Forecast	CRPS (mm)	MAE (mm)	Coverage (%)	Av.width (mm)
CSG-GEV	2.243	3.017	79.93	8.476
SLP	2.246	3.018	79.60	7.866
LP	2.245	3.017	79.90	8.471
CSG	2.252	3.019	80.24	8.350
GEV	2.283	3.033	79.66	8.683
Ensemble	2.929	3.708	67.95	8.599

Table 6: Mean CRPS of probabilistic forecasts, MAE of median forecasts and coverage and average width of 77.78 % central prediction intervals for the UWME data.

Forecast	CSG-GEV	SLP	LP	CSG	GEV	Ensemble
CSG-GEV	–	-0.802	-1.355	<b>-3.751</b>	<b>-8.805</b>	<b>-28.385</b>
SLP	0.157	–	0.295	-0.871	<b>-5.839</b>	<b>-25.650</b>
LP	0.311	-0.123	–	<b>-2.946</b>	<b>-9.450</b>	<b>-29.358</b>
CSG	1.128	0.175	0.785	–	<b>-5.237</b>	<b>-29.265</b>
GEV	<b>2.477</b>	1.898	<b>2.607</b>	1.631	–	<b>-26.845</b>
Ensemble	<b>21.869</b>	<b>19.342</b>	<b>21.791</b>	<b>21.967</b>	<b>20.504</b>	–

Table 7: Values of the test statistics of the DM test for equal predictive performance based on the CRPS (*upper triangle*) and the AE of the median forecast (*lower triangle*) for precipitation accumulation for the UWME data. Negative/positive values indicate a superior predictive performance of the forecast given in the row/column label, bold numbers correspond to values of the test statistic that are significant at the 0.05 level.

the earlier work of Baran and Nemoda (2016). As discussed in Section 3.4, a full mixture model (3.8) cannot be successfully estimated.

Given the individual CSG and GEV component models, the weight parameter of the novel two-step combination approach as well as the parameters of the SLP and LP models are estimated in a second step as described above for wind speed.

#### 4.3.1 University of Washington mesoscale ensemble

Figure 4 shows the verification rank histogram of the raw UWME predictions of precipitation and PIT histograms of the post-processed forecasts. Compared to the corresponding wind speed forecasts the ensemble predictions show slightly better calibration, but still exhibit clear deviations from the desired uniform distribution given by a systematic over-estimation of low precipitation accumulation values. All post-processing approaches clearly improve the calibration, however, the individual CSG EMOS model is slightly less calibrated compared to the GEV model and the different forecast combination approaches. These visual impressions

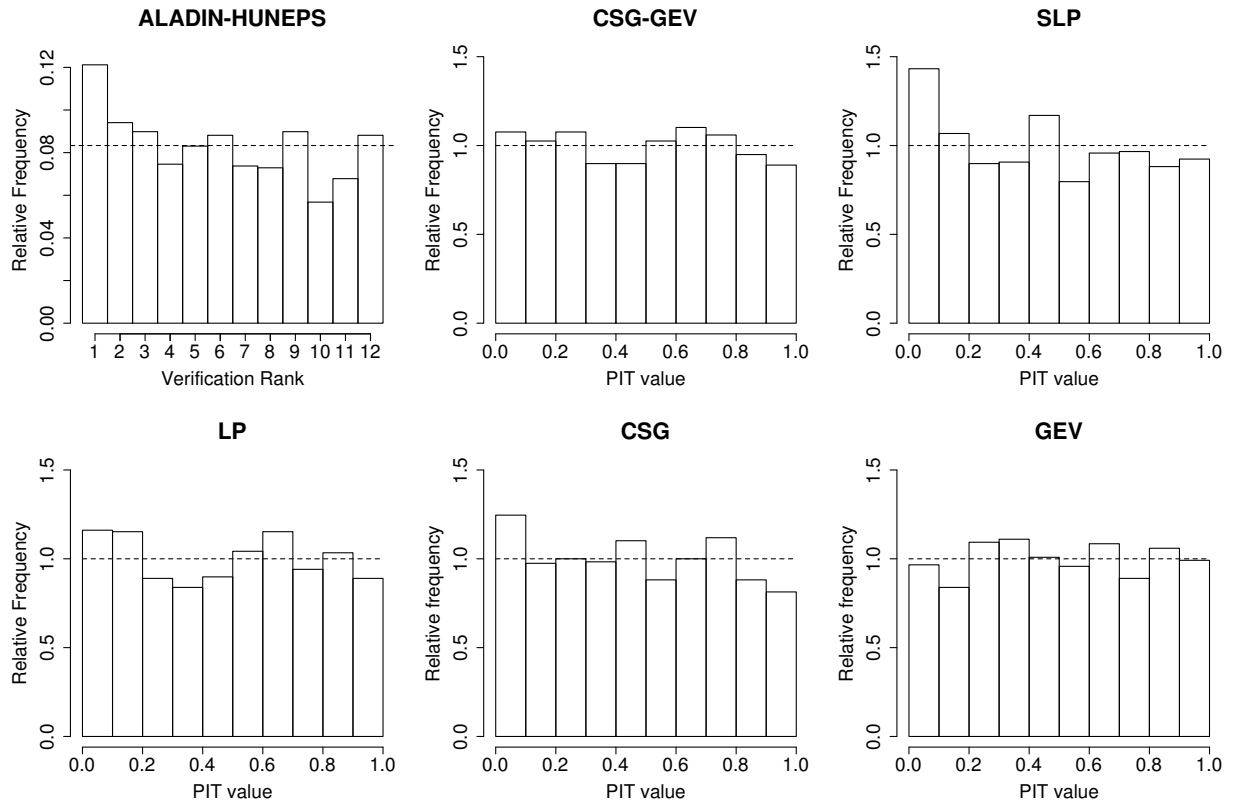


Figure 5: Verification rank histogram of the raw ensemble and PIT histograms of post-processed forecasts for precipitation accumulation for the ALADIN-HUNEPS data for the verification period 27 November 2010 – 25 March 2011.

are in line with the  $p$ -values of Kolmogorov-Smirnov tests of uniformity of the PIT values, see Table 1.

Verification scores of the different post-processing approaches are reported in Table 6. Not surprisingly, all post-processing approaches are clearly able to improve the ensemble predictions. The three forecast combination methods outperform the individual CSG and GEV component models, and the novel two-step CSG-GEV combination approach shows the lowest mean CRPS and MAE values. The values of the DM test statistics shown in Table 7 indicate that the score differences to the EMOS models based in single parametric distributions are significant at the 0.05 level, whereas the differences among the forecast combination approaches are not.

### 4.3.2 ALADIN-HUNEPS ensemble

Compared to all previously investigated data sets, the precipitation accumulation predictions of the ALADIN-HUNEPS ensemble are much better calibrated, see Figure 5. The different post-processing models are still able to correct for some of the deficiencies and result in

Forecast	CRPS (mm)	MAE (mm)	Coverage (%)	Av.width (mm)
CSG-GEV	0.465	0.638	87.54	2.198
SLP	0.477	0.647	87.97	2.130
LP	0.468	0.637	88.47	2.141
CSG	0.465	0.636	89.32	2.185
GEV	0.477	0.641	86.44	2.192
Ensemble	0.485	0.640	84.24	2.436

Table 8: Mean CRPS of probabilistic forecasts, MAE of median forecasts and coverage and average width of 83.33 % central prediction intervals for the ALADIN-HUNEPS ensemble.

Forecast	CSG-GEV	SLP	LP	CSG	GEV	Ensemble
CSG-GEV	–	-1.457	-0.829	0.035	<b>-2.622</b>	<b>-2.316</b>
SLP	0.902	–	0.173	1.841	0.012	-0.823
LP	-0.777	-1.017	–	1.326	<b>-2.822</b>	<b>-2.447</b>
CSG	-0.818	-1.148	-0.479	–	<b>-2.758</b>	<b>-2.928</b>
GEV	0.708	-0.561	0.805	0.799	–	-1.177
Ensemble	0.088	-0.410	0.182	0.246	-0.078	–

Table 9: Values of the test statistics of the DM test for equal predictive performance based on the CRPS (*upper triangle*) and the AE of the median forecast (*lower triangle*) for precipitation accumulation for the ALADIN-HUNEPS ensemble. Negative/positive values indicate a superior predictive performance of the forecast given in the row/column label, bold numbers correspond to values of the test statistic that are significant at the 0.05 level.

slightly better calibrated forecast distributions, except for the SLP approach which shares the systematic over-prediction of low precipitation accumulation values observed in the raw ensemble predictions. The worse calibration of the SLP forecast distributions can also be seen from the  $p$ -values of the Kolmogorov-Smirnov tests of uniformity in Table 1, where the SLP approach is the only post-processing model for which the null hypothesis of uniformity of the PIT values is rejected at the 0.05 level.

Verification scores for the ALADIN-HUNEPS ensemble predictions and the post-processing approaches are reported in Table 8. Here the EMOS model based on a single CSG distribution shows the best predictive performance. The different forecast combination approaches are unable to improve the forecasts of the CSG method, potentially due to the comparatively worse predictive performance of the GEV component model. While the two-step CSG-GEV combination approach introduced in Section 3.4 shows similar predictive performance to the CSG model, the SLP approach is unable to outperform the GEV component model. However, as indicated by DM tests of equal predictive performance, only the score differences of all models (except for the SLP approach) to the GEV model are significant at the 0.05 level,

	Wind speed					
	TN-LN (2 st)	TN-LN (ML)	SLP	LP	TN	LN
UWME	4.10	5.62	259.30	23.58	1.88	1.47
ALADIN-HUNEPS	0.23	0.31	31.90	2.66	0.09	0.06
	Precipitation accumulation					
	CSG-GEV	SLP	LP	CSG	GEV	
UWME	47.02	412.85	76.14	37.14	6.37	
ALADIN-HUNEPS	2.09	35.19	3.92	1.16	0.41	

Table 10: Median computation times (in seconds) required for estimating the various post-processing models for individual days in the corresponding verification period. The computation time required for estimating the individual component models is included in the reported values for the novel two-step combination approach as well as the SLP and the LP combination methods.

see Table 9.

#### 4.4 Computational aspects

The results of the four case studies summarized above indicate that the different forecast combination approaches are generally able to outperform the individual component models, and show similar predictive performance to the full mixture model in case of wind speed. An exception is given by the SLP approach which often even fails to outperform the worse of the two component models. A major benefit of the new two-step combination approach proposed in Section 3.4 compared to the LP and the full mixture model is given by the substantially lower computational costs to be discussed here. All computational times reported in this section are obtained using a standard laptop with an Intel Core i7-4800 MQ (4×2.70 GHz) CPU, 16 GB RAM and a Linux Mint 64 Bit operating system.

Table 10 shows the median of the computation times over the days in the verification period for the different post-processing models. The computation times of all forecast combination methods include the computation times of the individual component models. Compared to the proposed two-step combination approach, the computation times of the LP combination method are 6-11 times higher for wind speed, and 1.6-1.9 times higher for precipitation. For the SLP approach, the computation costs are much higher, and between 9 and 138 times longer compared to the two-step combination method. The full mixture model (3.3) for wind speed generally shows slightly better predictive performance in the case studies, however, it is computationally less efficient and requires around 35% longer computation times than the two-step combination approach.

The reduction in computational costs in the new two-step combination approach com-



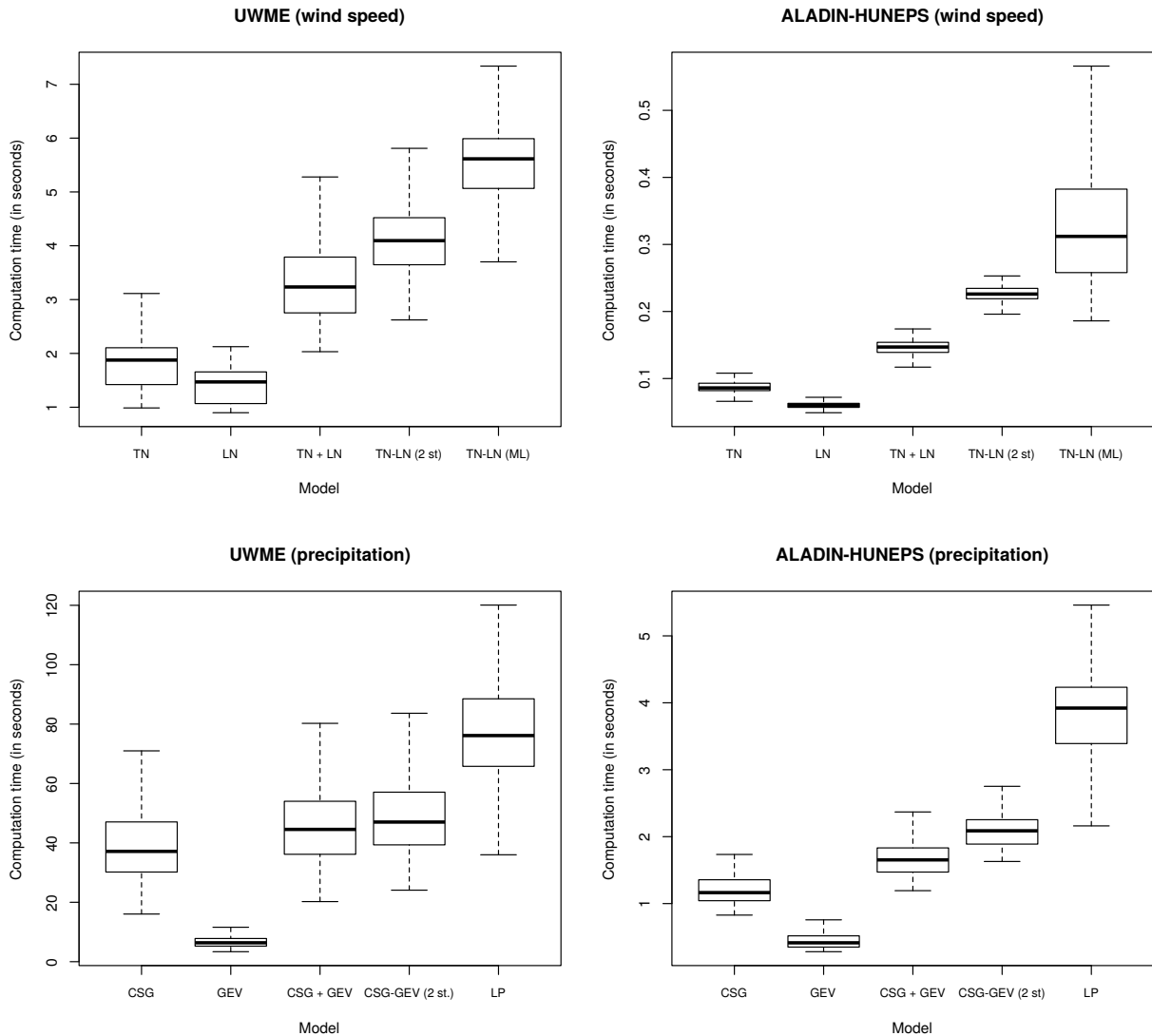


Figure 6: Distribution of computation times over days in the verification period for the different EMOS models and combination approaches. TN+LN and CSG+GEV refers to the sum of the computation times required for estimating the respective component models. The computation times of the LP approach are omitted in the top row due to the substantially higher values, see Table 10.

pared to the SLP and LP methods is achieved by obtaining the weight parameter in an efficient way without repeated numerical integrations for all parameter values in a candidate set. Compared to the full mixture model for wind speed, the parameter estimation of the individual model and the weight is more efficient, as fewer parameters have to be estimated since the estimation is not performed jointly over all parameters.

Figure 6 further graphically illustrates the distribution of the computation times of the

different post-processing approaches. It can be observed that the novel two-step combination approach only requires relatively small additional computation time compared to the estimation of the individual component models, whereas both the full mixture model for wind speed and the LP combination models require clearly more computational resources. However, all computation times reported here are generally much lower compared to the computational costs of generating the ensemble forecasts.

## 5 Conclusions

We have proposed a novel, computationally efficient approach to combining forecast distributions from individual post-processing models. The proposed method is a two-step procedure, where in a first step individual EMOS models based on single parametric distributions are estimated. Given the model estimates, the forecast distributions are then combined in the form of a weighted mixture, where the weight is determined in a single numerical integration step.

In four case studies the proposed combination approach outperforms the individual component models and shows similar predictive performance compared to the standard linear pool and to a full mixture model for wind speed. However, the computational costs are significantly lower and, given the availability of suitable component models, the proposed methodology can be applied to any weather variable of interest. Therefore, it is also useful for quantities such as precipitation, where full mixture models cannot be estimated successfully. Applications of the proposed combination method to further weather variables such as total cloud cover (Hemri *et al.*, 2016) might be an interesting starting point for future research. Generally, the proposed methodology could be extended to more than two mixture components, however, the computational costs will increase with number of mixture components due to the larger number of required numerical integration steps.

Regarding the relative predictive performance of the different forecast combination methods in the case studies, the SLP approach generally performs worse than the proposed two-step approach and it is rarely able to outperform the individual component models. By contrast, it showed promising results in Möller and Groß (2016), where, however, the combined forecast distributions exhibited very different and complementary calibration properties with overdispersive forecast from one model, and underdispersive forecasts from the other one, which is not the case in any of our case studies.

Other forecast combination approaches have been proposed in the literature including for example the beta-transformed linear pool (Gneiting and Ranjan, 2013) or Bayesian generalizations thereof (Bassetti *et al.*, 2015). These combination approaches provide an interesting starting point for future research, however, their applicability might be limited by high computational costs.

Further, an alternative approach to combining forecast distributions is given by using

suitably weighted proper scoring rules that emphasize certain regions of interest. Thereby, the forecast combination weight can be determined by which of the competing distributions performs better for certain region of interest, see Lerch *et al.* (2015) for details.

An entirely different approach to post-processing that completely circumvents the problem of choosing suitable parametric forecast distributions is the use of non-parametric methods, see for example Hamill and Whitaker (2006); Flowerdew (2014), and Taillardat *et al.* (2016). However, these approaches suffer from the limitation that the support of the forecast distribution is necessarily restricted to the range of observed values in the training sets. Further, these methods require sufficiently long training periods, and generally lead to high computational costs.

**Acknowledgments.** Essential part of the work leading to this paper was made during the visit of Sándor Baran at the Heidelberg Institute for Theoretical Studies in the framework of the visiting scientist program. Sándor Baran was also supported by the János Bolyai Research Scholarship of the Hungarian Academy of Sciences. Sebastian Lerch gratefully acknowledges support by Deutsche Forschungsgemeinschaft (DFG) through the project ‘C7 – Statistical post-processing and stochastic physics for ensemble predictions’ within Transregional Collaborative Research Center 165 ‘Waves to Weather’, and thanks the Klaus Tschira Foundation for infrastructural support at the Heidelberg Institute for Theoretical Studies. The authors further thank the University of Washington MURI group for providing the UWME data and Mihály Szűcs from the HMS for providing the ALADIN-HUNEPS data.

## References

- Baran, S. and Lerch, S. (2015) Log-normal distribution based EMOS models for probabilistic wind speed forecasting. *Q. J. R. Meteorol. Soc.* **141**, 2289–2299.
- Baran, S. and Lerch, S. (2016) Mixture EMOS model for calibrating ensemble forecasts of wind speed. *Environmetrics* **27**, 116–130.
- Baran, S. and Nemoda, D. (2016) Censored and shifted gamma distribution based EMOS model for probabilistic quantitative precipitation forecasting. *Environmetrics* **27**, 280–292.
- Bassetti, F., Casarin, R. and Ravazzolo, F. (2015) Bayesian nonparametric calibration and combination of predictive distributions *University Ca’ Foscari of Venice, Dept. of Economics Research Paper Series* No. 04/WP/2015. Available from: [http://papers.ssrn.com/sol3/papers.cfm?abstract\\_id=2566304](http://papers.ssrn.com/sol3/papers.cfm?abstract_id=2566304) [Accessed on 22 July 2016]
- Descamps, L., Labadie, C., Joly, A., Bazile, E., Arbogast, P. and Cébron, P. (2015) PEARP, the Météo-France short-range ensemble prediction system. *Q. J. R. Meteorol. Soc.* **141**, 1671–1685.

- Diebold F. X. and Mariano, R. S. (1995) Comparing predictive accuracy. *J. Bus. Econ. Stat.* **13**, 253–263.
- Eckel, F. A. and Mass, C. F. (2005) Effective mesoscale, short-range ensemble forecasting. *Wea. Forecasting* **20**, 328–350.
- Flowerdew, J. (2014) Calibrating ensemble reliability whilst preserving spatial structure *Tellus A* **66**, 22662.
- Fraley, C., Raftery, A. E. and Gneiting, T. (2010) Calibrating multimodel forecast ensembles with exchangeable and missing members using Bayesian model averaging. *Mon. Weather Rev.* **138**, 190–202.
- Garcia, A., Torres, J. L., Prieto, E. and De Francisco, A. (1998) Fitting wind speed distributions: A case study. *Sol. Energ.* **62**, 139–144.
- Gneiting, T. (2014) Calibration of medium-range weather forecasts. *ECMWF Technical Memorandum* No. 719. Available from: <http://www.ecmwf.int/sites/default/files/elibrary/2014/9607-calibration-medium-range-weather-forecasts.pdf> [Accessed on 22 July 2016]
- Gneiting, T., Balabdaoui, F. and Raftery, A. E. (2007) Probabilistic forecasts, calibration and sharpness. *J. Roy. Stat. Soc. B.* **69**, 243–268.
- Gneiting, T. and Raftery, A. E. (2005) Weather forecasting with ensemble methods. *Science* **310**, 248–249.
- Gneiting, T. and Raftery, A. E. (2007) Strictly proper scoring rules, prediction and estimation. *J. Amer. Statist. Assoc.* **102**, 359–378.
- Gneiting, T., Raftery, A. E., Westveld, A. H. and Goldman, T. (2005) Calibrated probabilistic forecasting using ensemble model output statistics and minimum CRPS estimation. *Mon. Wea. Rev.* **133**, 1098–1118.
- Gneiting, T. and Ranjan, R. (2013) Combining predictive distributions. *Electron. J. Stat.* **7**, 1747–1782.
- Good, I. J. (1952) Rational decisions. *J. Roy. Stat. Soc. B* **14**, 107–114.
- Grell, G. A., Dudhia, J. and Stauffer, D. R. (1995) A description of the fifth-generation Penn state/NCAR mesoscale model (MM5). *Technical Note* NCAR/TN-398+STR. National Center for Atmospheric Research, Boulder. Available at: <http://www2.mmm.ucar.edu/mm5/documents/mm5-desc-doc.html> [Accessed on 22 July 2016]
- Hamill, T. M. and Whitaker, J. S. (2006) Probabilistic quantitative precipitation forecasts based on reforecast analogs: Theory and application. *Mon. Wea. Rev.* **134**, 3209–3229.

- Hemri, S., Haiden, T. and Pappenberger, F. (2016) Discrete post-processing of total cloud cover ensemble forecasts. *Mon. Wea. Rev.*, in press.
- Horányi, A., Kertész, S., Kullmann, L. and Radnóti, G. (2006) The ARPEGE/ALADIN mesoscale numerical modeling system and its application at the Hungarian Meteorological Service. *Időjárás* **110**, 203–227.
- Horányi, A., Mile, M. and Szűcs, M. (2011) Latest developments around the ALADIN operational short-range ensemble prediction system in Hungary. *Tellus A* **63**, 642–651.
- Iversen, T., Deckmin, A., Santos, C., Sattler, K., Bremnes, J. B., Feddersen, H. and Frogner, I.-L. (2011) Evaluation of 'GLAMEPS' – a proposed multimodel EPS for short range forecasting. *Tellus A* **63**, 513–530.
- Jordan, A., Krüger, F., and Lerch, S. (2016) *scoringRules: Scoring Rules for Parametric and Simulated Distribution Forecasts*. Available at <https://cran.r-project.org/web/packages/scoringRules> [Accessed on 22 July 2016]
- Justus, C. G., Hargraves, W. R., Mikhail, A. and Graber, D. (1978) Methods for estimating wind speed frequency distributions. *J. Appl. Meteor.* **17**, 350–353.
- Lerch, S. and Baran, S. (2016) Similarity-based semilocal estimation of post-processing models. *J. Roy. Stat. Soc. C*, doi:10.1111/rssc.12153.
- Lerch, S. and Thorarinsdottir, T. L. (2013) Comparison of non-homogeneous regression models for probabilistic wind speed forecasting. *Tellus A* **65**, 21206.
- Lerch, S., Thorarinsdottir, T. L., Ravazzolo, F. and Gneiting, T. (2015) Forecaster's dilemma: Extreme events and forecast evaluation. arXiv:1512.09244. Available from <http://arxiv.org/abs/1512.09244> [Accessed on 22 July 2016]
- Matheson, J. E. and Winkler, R. L. (1976) Scoring rules for continuous probability distributions. *Manag. Sci.* **22**, 1087–1096.
- Molteni, F., Buizza, R., Palmer, T. N. and Petroliagis, T. (1996) The ECMWF ensemble prediction system: Methodology and validation. *Q. J. R. Meteorol. Soc.* **122**, 73–119.
- Möller, A. and Groß, J. (2016) Probabilistic temperature forecasting based on an ensemble AR modification *Q. J. R. Meteorol. Soc.* **142**, 1385–1394.
- National Weather Service (1998) *Automated Surface Observing System (ASOS) Users Guide*. Available at: <http://www.weather.gov/asos/aum-toc.pdf> [Accessed on 22 July 2016]
- Nelder, J. A. and Mead, R. (1965) A simplex algorithm for function minimization. *Comput. J.* **7**, 308–313.

- Palmer, T. N. (2002) The economic value of ensemble forecasts as a tool for risk assessment: From days to decades. *Q. J. R. Meteorol. Soc.* **128**, 747–774.
- Press, W. H., Teukolsky, S. A., Vetterling, W. T. and Flannery, B. T. (2007) *Numerical Recipes 3rd Edition: The Art of Scientific Computing*. Cambridge University Press, Cambridge.
- R Core Team (2016) *R: A Language and Environment for Statistical Computing*. <https://www.R-project.org/> [Accessed on 22 July 2016]
- Raftery, A. E., Gneiting, T., Balabdaoui, F. and Polakowski, M. (2005) Using Bayesian model averaging to calibrate forecast ensembles. *Mon. Wea. Rev.* **133**, 1155–1174.
- Scheuerer, M. (2014) Probabilistic quantitative precipitation forecasting using ensemble model output statistics. *Q. J. R. Meteorol. Soc.* **140**, 1086–1096.
- Scheuerer, M. and Hamill, T. M. (2015) Statistical post-processing of ensemble precipitation forecasts by fitting censored, shifted gamma distributions. *Mon. Wea. Rev.* **143**, 4578–4596.
- Scheuerer, M. and Möller, D. (2015) Probabilistic wind speed forecasting on a grid based on ensemble model output statistics. *Ann. Appl. Stat.* **9**, 1328–1349.
- Sloughter, J. M., Raftery, A. E., Gneiting, T. and Fraley, C. (2007) Probabilistic quantitative precipitation forecasting using Bayesian model averaging. *Mon. Wea. Rev.* **135**, 3209–3220.
- Swinbank, R., Kyouda, M., Buchanan, P., Froude, L., Hamill, T. M., Hewson, T. D., Keller, J. H., Matsueda, M., Methven, J., Pappenberger, F., Scheuerer, M., Titley, H. A., Wilson, L. and Yamaguchi, M. (2016) The TIGGE project and its achievements. *B. Am. Meteorol. Soc.* **97**, 49–67.
- Taillardat, M., Mestre, O., Zamo, M. and Naveau, P. (2016) Calibrated ensemble forecasts using quantile regression forests and ensemble model output statistics. *Mon. Wea. Rev.*, in press.
- Thorarinsdottir, T. L. and Gneiting, T. (2010) Probabilistic forecasts of wind speed: Ensemble model output statistics by using heteroscedastic censored regression. *J. Roy. Statist. Soc. Ser. A* **173**, 371–388.
- Wilks, D. S. (2011) *Statistical Methods in the Atmospheric Sciences*. 3rd ed., Elsevier, Amsterdam.